

# THE LOW VELOCITY WIND FROM THE CIRCUMSTELLAR MATTER AROUND THE B9V STAR $\sigma$ HERCULIS

C. H. CHEN & M. JURA

Department of Physics and Astronomy, University of California, Los Angeles, CA 90095-1562;

cchen@astro.ucla.edu; jura@clotho.astro.ucla.edu

*Draft version November 4, 2018*

## ABSTRACT

We have obtained *FUSE* spectra of  $\sigma$  Her, a nearby binary system, with a main sequence primary, that has a Vega-like infrared excess. We observe absorption in the excited fine structure lines C II\* at 1037 Å, N II\* at 1085 Å, and N II\*\* at 1086 Å that are blueshifted by as much as  $\sim$ 30 km/sec with respect to the star. Since these features are considerably narrower than the stellar lines and broader than interstellar features, the C II and N II are circumstellar. We suggest that there is a radiatively driven wind, arising from the circumstellar matter, rather than accretion as occurs around  $\beta$  Pic, because of  $\sigma$  Her's high luminosity. Assuming that the gas is liberated by collisions between parent bodies at 20 AU, the approximate distance at which blackbody grains are in radiative equilibrium with the star and at which 3-body orbits become unstable, we infer  $dM/dt \sim 6 \times 10^{-12} M_{\odot} \text{ yr}^{-1}$ . This wind depletes the minimum mass of parent bodies in less than the estimated age of the system.

*Subject headings:* stars: individual ( $\sigma$  Herculis) — circumstellar matter — planetary systems: formation

## 1. INTRODUCTION

Planets are believed to form within circumstellar disks around young main sequence stars (with ages  $\leq$ 100 Myr) composed of dust and gas (Beckwith & Sargent 1996). Dusty circumstellar disks, with radii comparable to the distance between the Sun and the Kuiper Belt, have been imaged around several young, nearby main sequence stars (Schneider et al. 1999, Weinberger et al. 1999, Holland et al. 1998). However, few studies have focused on the properties of gas and dust at a few AU from main sequence stars where the temperature of parent bodies may reach  $\sim$ 300 K (Chen & Jura 2001, Heap et al. 2000, Low et al. 1999). At these distances, ice sublimates and large solids may evolve into terrestrial planets. We have carried out a far ultraviolet study of gas around a main sequence star, which possess a possible 10  $\mu\text{m}$  excess attributed to dust with a grain temperature ( $T_{gr} \sim 300$  K), to learn about the physical processes in the regions where terrestrial planets may have formed or may be forming.

$\sigma$  Herculis is a binary system, at a distance 93 pc away from the Sun (see Table 1), with a B9V primary and a companion at a projected separation of 0.07'' (Hartkopf et al. 1997). The spectral type of the companion has not been well determined. Astrometric estimates for the masses, using orbital parameters determined from speckle interferometry and relative brightness measurements from *Hipparcos*, yield  $M_1 = 3.0 \pm 0.7 M_{\odot}$ ,  $M_2 = 1.5 \pm 0.5 M_{\odot}$ , and  $M_{tot} = 4.5 \pm 0.8 M_{\odot}$  (Martin et al. 1998). The  $V - R$  color and the absolute  $V$ -band magnitude of the secondary are consistent with a classification of early-type A ( $\Delta m = 2.5 \pm 0.1$  mag for  $5000 \text{ \AA} < \lambda < 8500 \text{ \AA}$ ; Hummel et al. 2002). The age of  $\sigma$  Her has been estimated to be  $\sim$ 200 Myr based upon its  $uvby\beta$  photometry (Grosbøl 1978). If we apply a correction for the high rotational velocity of this star to the Strömgren photometry (Figueras & Blasi 1998), we find an estimated age of  $\sim$ 140  $\pm$  100 Myr for  $\sigma$  Her.

The  $\sigma$  Her binary system possess a mid infrared excess

indicative of the presence of dust ( $L_{IR}/L_* = 6.6 \times 10^{-5}$ ; Fajardo-Acosta, Telesco, & Knacke 1998). The dust appears to be divided into two populations. The colder grains were first discovered based upon measurements of a strong *IRAS* 60  $\mu\text{m}$  excess (Sadakane & Nishida 1986; Coté 1987) which is unresolved with *ISO* (Fajardo-Acosta, Stencel, & Backman 1997). Recent ground based photometry of  $\sigma$  Her suggests that this star may also possess 10  $\mu\text{m}$  and 20  $\mu\text{m}$  excesses (Fajardo-Acosta et al. 1998). The spectral energy distribution of this warmer dust population is marginally fit by blackbody grains with a temperature,  $T_{gr} \sim 300 \pm 100$  K, significantly warmer than  $T_{gr} \sim 100$  K grains observed with *IRAS* at 60  $\mu\text{m}$ . If the particles are blackbodies in radiative equilibrium with the binary, then the dust is located at a distance of between 7 AU and 30 AU, significantly closer than the 120 AU distance inferred for the cooler population.

While Vega-like systems, such as  $\sigma$  Her, possess dust, the gas:dust ratio is not well known. Recent ultraviolet searches for molecular hydrogen, using *FUSE*, have failed to detect any molecular hydrogen around the dusty main sequence stars  $\beta$  Pic (Lecavelier des Etangs et al. 2001) and 51 Oph (Roberge et al 2002). However, spectra of these systems possess time-variable, redshifted atomic gas features which are believed to be generated by the evaporation of infalling comets (Vidal-Madjar et al. 1994; Roberge et al. 2002). *IUE* observations of  $\sigma$  Her have revealed the presence of narrow time-variable Si II\*  $\lambda 1533.4$  absorption features which are blueshifted with respect to the heliocentric velocity of the star (-11 km/sec; Bruhweiler, Grady, & Chiu 1989) with a range of 2 to 21 km/sec (Grady et al. 1991). Although  $\sigma$  Her possess time-variable, velocity-shifted absorption features similar to  $\beta$  Pic, the high stellar luminosity and binary nature of the system may result in a different fate for gas liberated around  $\sigma$  Her compared with material liberated around  $\beta$  Pic.

## 2. OBSERVATIONS

Our data were obtained on 2001 July 15 using the *Far Ultraviolet Spectroscopic Explorer* (*FUSE*). Our observations were made in histogram mode, using the low resolution  $30'' \times 30''$  aperture which covers the wavelength range between 905 and 1187 Å. The *FUSE* satellite has four channels (LiF 1, SiC 1, LiF 2, SiC 2) which form two nearly identical “sides” (labeled 1 and 2) and each consist of a LiF grating, a SiC grating and, a detector. Each detector is divided into two independent segments (a and b), separated by a small gap. The eight partially overlapping spectra that fall on different portions of the two detectors (LiF 1a, LiF 1b, etc.) cover the entire wavelength range. A description of the on orbit performance of *FUSE* is described in (Sahnow et al. 2000) with a conservative estimate for the spectral resolution ( $R = \lambda/\Delta\lambda = 15000$ ) of the spectrograph. The data were calibrated at Johns Hopkins using the CALFUSE 2.0.5 pipeline.

We wavelength calibrate our data by cross correlating the spectrum of  $\sigma$  Her with a rotationally broadened synthetic stellar spectrum (Chayer 2001) in order to determine the relative wavelength of the circumstellar lines with respect to the stellar lines. Since the synthetic spectrum (calculated for a star with solar metallicity,  $T_{eff} = 10,000$  K,  $\log g = 4.0$  and  $v \sin i = 270$  km/sec) fits the observed spectrum well in the region of the stellar C I absorption lines (which lie in the LiF 1B channel), we are able to set the “zero-point” wavelength calibration for the spectrum to within 15 km/sec. Since the LiF 1A and LiF 1B channels have the same wavelength shift, cross correlating the observed LiF 1B channel spectrum with the synthetic spectrum allows us to calculate the “zero-point” shift needed for both LiF 1A and LiF 1B. The offsets for the remaining channels analyzed (LiF 2B, SiC 1A, SiC 2B) are calculated by cross correlating these spectra with spectra from the LiF 1A channel in the wavelength regions in which they overlapped. The uncertainty in the relative wavelength calibration is dominated by detector distortions and is  $\sim 9$  km/sec. No circumstellar lines were detected at wavelengths within the SiC 2A/1B channels (905 Å to 1005 Å); thus, these channels are not discussed further in this paper.

All of our LiF 2A channel exposures of  $\sigma$  Her suffer from an effect called detector x-walk, in which low pulse height events are misplaced in the dispersion direction because of gain sag in the regions on the detector on which the brightest airglow lines fall. Currently, there is no correction for detector x-walk in the histogram data calibration pipeline; thus, we excluded all LiF 2A spectra from our analysis.

### 3. CIRCUMSTELLAR GASES

Absorption in the excited fine structure states, C II\* at 1037.02 Å, N II\* at 1084.58 Å, and N II\*\* at 1085.54 Å and 1085.70 Å are observed (see Figure 1a and 1b). Since these lines are significantly narrower than the rotationally broadened stellar lines and broader than the observed interstellar lines, shown for comparison in Figures 1c and 1a respectively, the gases are circumstellar. No circumstellar O I is detected toward  $\sigma$  Her.

We fit a model to each multiplet using a quadratic polynomial plus a Gaussian to represent the photospheric component and Gaussians to represent each of the narrow

circumstellar components. We initially fit the model by hand, masking out the narrow circumstellar lines and fitting the broad photospheric component and adding each circumstellar component back individually. Then, we ran a minimize  $\chi^2$  routine on the model using our initial fit as a starting point. In each model fit, we let the wavelength, scale, and FWHM for each Gaussian be free parameters in addition to the 3 coefficients for the quadratic polynomial. The model fits for the C II and N II features are overlaid on the spectra shown in Figures 1a and 1b and have  $\chi^2 = 0.77$  and 0.91 respectively. Changing the wavelength of the circumstellar features by 10 km/sec and 20 km/sec increases the reduced  $\chi^2$  of the fit to  $\sim 1.5$  and  $\sim 2.5$  respectively for C II and to  $\sim 1.4$  and  $\sim 2.4$  respectively for N II. We use the wavelengths from the fits of the narrow circumstellar cores to determine the velocity shift of the gas and the photosphere fit to estimate the continuum in our measurements of the equivalent widths. The excited N II\*\* appears blueshifted by 25–28 km/sec and the excited C II\* appears blueshifted by 20 km/sec. The line equivalent widths and their statistical uncertainties are given in Table 2. The population of all observed species in excited fine structure levels can be explained with radiative pumping by stellar ultraviolet photons.

We observed no absorption in the H<sub>2</sub> Lyman (5,0) band or the CO C-X (0,0) band toward this star. The  $3\sigma$  upper limits on the H<sub>2</sub> line-of-sight column densities in the  $J = 0$  and  $J = 1$  rotational levels are measured, from the P(1) and R(0) transitions at 1036.54 Å and 1038.16 Å, to be  $N(J = 0) \leq 4 \times 10^{14}$  cm<sup>-2</sup> and  $N(J = 1) \leq 7 \times 10^{14}$  cm<sup>-2</sup> using wavelengths and oscillator strengths from Abgrall et al (1993). The  $3\sigma$  upper limits on the CO line-of-sight column densities in the  $J = 2$  and  $J = 4$  rotational levels are measured, from the P(3) and R(3) transitions at 1088.05 Å and 1087.73 Å, to be  $N(J = 2) \leq 1.4 \times 10^{14}$  cm<sup>-2</sup> and  $N(J = 4) \leq 1.0 \times 10^{14}$  cm<sup>-2</sup> using wavelengths and oscillator strengths from Morton & Noreau (1994). The upper limits on the column density of CO in the  $J = 2$  and  $J = 4$  levels suggest that  $N(CO) \leq 5 \times 10^{14}$  cm<sup>-2</sup> or  $N(CO) \leq 7 \times 10^{14}$  cm<sup>-2</sup> for excitation temperatures of 25 K and 100 K respectively.

### 4. PARENT BODIES

The observation of mid infrared excess associated with  $\sigma$  Her suggests the presence of micron-sized grains around this star. We hypothesize that the circumstellar gas detected around  $\sigma$  Her is physically associated with the dust in ways described below.

Since  $\sigma$  Her is a B9V star, radiation pressure will effectively remove small grains from the environment around the star. A lower limit to the size of dust grains orbiting a star can be found by balancing the force due to radiation pressure with the force due to gravity. For small grains with radius  $a$ , the force due to radiation pressure overcomes gravity for:

$$a < 3L_* Q_{pr} / (16\pi GM_{tot}c\rho_s) \quad (1)$$

(Artymowicz 1988) where  $L_*$  is the stellar luminosity,  $M_{tot}$  is the binary mass,  $Q_{pr}$  is the radiation pressure coupling coefficient, and  $\rho_s$  is the density of an individual grain. Since radiation from a late B-type star is dominated by optical and ultraviolet light, we expect that  $2\pi a/\lambda \gg 1$  and therefore the effective cross section of the grains can be

approximated by their geometric cross section so  $Q_{pr} \approx 1$ . We estimate the stellar luminosity from the bolometric magnitude using the *Hipparcos* V-band magnitude ( $m_V = 4.01$  mag), correcting for the interstellar extinction measured along the line of sight ( $E(B-V) = 0.06$ ; Fajardo-Acosta et al. 1998) using the far ultraviolet extinction law derived in Cardelli, Clayton, & Mathis (1989), a distance 93 pc, and a bolometric correction (Flower 1996) corresponding to an effective temperature  $T_{eff} = 10,500$  K. For the primary, we estimate a stellar luminosity  $L_* = 230 L_\odot$ . We similarly estimate the luminosity for the secondary assuming a relative magnitude  $\delta m = 2.5$  mag and a bolometric correction corresponding to an effective temperature of  $T_{eff} = 9530$  K. For the secondary, we find  $L_* = 7.4 L_\odot$ . Thus, the contribution of the secondary to the total luminosity of the system is small and can be neglected. The mass of the binary system has been determined astrometrically ( $M_{tot} = 4.5 \pm 0.8 M_\odot$ ; Martin et al. 1998). For circumstellar dust grains around  $\sigma$  Her with a density  $\rho_s = 2.5 \text{ g cm}^{-3}$ , we find a minimum grain radius of  $a = 15 \mu\text{m}$ ; thus, the grains are large enough to act as black bodies. Grains smaller than  $15 \mu\text{m}$  will be effectively removed by radiation pressure on a timescale of  $< 10$  years.

Another mechanism which may remove particles from the circumstellar environment is Poynting-Robertson drag. The Poynting-Robertson lifetime of grains in a circular orbit, a distance  $D_{in}$  from a star is

$$t_{PR} = \left( \frac{4\pi a \rho_s}{3} \right) \frac{c^2 D_{in}^2}{L_*} \quad (2)$$

(Burns et al. 1979). With the parameters given above and  $D_{in} = 20 \text{ AU}$ , the Poynting-Robertson lifetime of the grains is  $t_{PR} = 4.6 \times 10^4$  years. Since this timescale is significantly shorter than the stellar age,  $t_{age}$ , we hypothesize that the grains are replenished through collisions between larger bodies. It is difficult to provide an accurate estimate of the true mass in parent bodies. Since  $\sigma$  Her has an age of  $\sim 140$  Myr, objects with a radius larger than 4.5 cm will not have had enough time to spiral into the star under Poynting-Robertson drag. Large masses of circumstellar dust could exist around  $\sigma$  Her and be difficult to detect at mid infrared wavelengths because large grains have relatively less surface area compared to their mass.

We can estimate a lower limit for the total mass contained in parent bodies around  $\sigma$  Her assuming that the system is in a steady state. If  $M_{PB}$  denotes the mass in parent bodies, then we may write

$$M_{PB} \geq \frac{4L_{IR}t_{age}}{c^2} \quad (3)$$

(Chen & Jura 2001). Assuming that the binary system  $\sigma$  Her has a fractional infrared luminosity  $L_{IR}/L_* = 6.6 \times 10^{-5}$  (Fajardo-Acosta et al. 1998) and an age  $t_{age} = 140$  Myr, we find a minimum mass in parent bodies of  $M_{PB} \geq 0.20 M_\oplus$ . By analyzing the composition of the circumstellar gas, we can infer the properties of the parent bodies.

## 5. THE WIND FROM THE CIRCUMSTELLAR MATTER

The approximation that the gas is optically thin is probably not valid for the C II. If the atoms were optically thin, then the ratio of their equivalent widths,

$W_\lambda(\text{C II})/W_\lambda(\text{C II}^*)$ , would be 0.50, assuming the excitation temperature is  $\gg 100$  K. However, from our *FUSE* spectra, we measure  $W_\lambda(\text{C II})/W_\lambda(\text{C II}^*) = 0.83$ . We estimate the optical depths of the atoms in the ground state and first excited state from the ratio of the measured equivalent widths, assuming normalized Gaussian line profiles.

$$\phi(\Delta\nu) = \frac{1}{\Delta\nu_o \sqrt{\pi}} \exp\left(\frac{-\Delta\nu^2}{\Delta\nu_o^2}\right) \quad (4)$$

where  $\Delta\nu_o$  is the line width. The equivalent width of a line with a Gaussian profile is

$$\frac{W_\lambda}{\lambda} = \frac{2\Delta\nu_o F(\tau_o)}{\nu_o} \quad (5)$$

where

$$F(\tau_o) = \int_0^\infty \left[ 1 - \exp(-\tau_o e^{-x^2}) \right] dx \quad (6)$$

(Spitzer 1978) and  $\tau_o$  is the optical depth at line center. We estimate  $\tau_o$  for C II and C II\*, assuming that  $\tau_o(\text{C II})/\tau_o(\text{C II}^*) = 0.5$  and using the observational result that  $F(\tau_o(\text{C II}))/F(\tau_o(\text{C II}^*)) = 0.83$ . For C II and C II\*, we estimate  $\tau_o = 3.8$  and  $\tau_o = 7.6$  respectively and  $\Delta\nu_o = 2.0 \times 10^{11} \text{ Hz}$ . In Table 2, we estimate the column densities of C II and N II using the equivalent widths given in Table 2 and wavelengths and oscillator strengths from Morton (1991), assuming that the N II is optically thin and that the C II has the optical depths given above and is located at the edge of the cloud. It is difficult to determine the optical depth of the N II lines because the N II\* and N II\*\* lines, which are observed with *FUSE*, are doublet and triplet blends. High resolution spectroscopy is needed to determine the detailed characteristics of the gas.

Whether atomic gas is expected to fall into the star or to be blown out of the circumstellar environment can be determined from  $\beta = F_{rad}/F_{grav}$ . We calculate the ratio of the force due to radiation pressure to the force due to gravity for the observed atomic species assuming that the N II is optically thin and the C II has the optical depth given above and is at the edge of the cloud. The force due to radiation pressure acting on the atoms is given by the following expression:

$$F_{rad} = \sum_{\text{all transitions}} \frac{\pi e^2}{m_e c^2} f_i G_i(\tau) \Phi_{o_i}, \quad (7)$$

where  $f_i$  is the absorption oscillator strength,  $\Phi_{o_i}$  is the flux of photons arriving at the distance of the atom from the star, and  $G(\tau)$  is the line shielding function.

$$G(\tau) = \int_{-\infty}^{\infty} \phi(\Delta\nu) \frac{\Phi_\nu(\Delta\nu)}{\Phi_o} d(\Delta\nu) \quad (8)$$

where  $\Phi_\nu(\Delta\nu)$  is the flux in the cloud at  $\Delta\nu$ .

$$\Phi_\nu(\Delta\nu) = \Phi_o \exp(-\tau(\Delta\nu)) \quad (9)$$

If the gas is optically thin at all frequencies, then  $G(\tau) = 1.0$ . We use an approximation for  $G(\tau)$  given by Federman, Glassgold, & Kwan (1979). For  $\tau = 3.8$  and 7.6,  $G(\tau) = 0.12$  and  $G(\tau) = 0.051$  respectively. We infer  $\Phi_{o_i}$  from our *FUSE* spectra and from archival *IUE* spectra at longer wavelengths. Correcting for interstellar extinction, as described in section 4, suggests that the stellar flux is 2.3 and 2.1 times brighter than observed by *FUSE* at the

C II and N II line wavelengths respectively. The estimated values for  $\beta$  are listed in Table 2. The radiation pressure for the ground state and excited N II is generated by transitions in the *FUSE* wavelength range while the radiation pressure for the ground state and excited C II is dominated by high f-value transitions at  $\sim 1300$  Å where the stellar flux is significantly stronger. For C II and N II atoms around  $\sigma$  Her,  $\beta > 1$  suggesting that the high luminosity of the B9V primary effectively removes circumstellar gas from this system in a low velocity wind.

We can calculate the outflow velocity for atomic gas around  $\sigma$  Her assuming that radiation pressure and gravity act on the gas and making the simplification that the atoms begin from rest. Since radiation pressure and gravity are the only forces acting on the gas once it is released from the parent bodies, the gas is expected to be on a hyperbolic orbit. We derive an expression for the outflow velocity,  $v_\infty$ , from the equation for the force acting on the gas. If the gas is low density so that collisions are unimportant, then the outflow velocity,  $v_\infty$ , for  $\beta \geq 1$ , is

$$v_\infty = \left[ \sum_{\text{all transitions}} \frac{G_i(\tau) L_{\nu_i} e^2 f_i}{2 D_{in} m_e c^2 m_{atom}} \left(1 - \frac{1}{\beta}\right) \right]^{\frac{1}{2}} \quad (10)$$

where  $m_{atom}$  is the mass of the atomic species. For all the observed states of N II, the outflow velocity of atomic gas blown out of this system is  $v_\infty = 24 - 26$  km/sec, assuming  $D_{in} = 20$  AU and that the gas is optically thin. For C II and C II\*, the predicted outflow velocities are  $v_\infty = 29$  km/sec and  $v_\infty = 31$  km/sec respectively, assuming  $D_{in} = 20$  AU and that the gas is at the edge of the cloud. These velocities are in rough agreement with the observed blueshifts of C II\* and N II\*\*.

We can estimate the gas masses entrained in the wind around  $\sigma$  Her based upon the measurements of the column densities and the escape velocities for the atomic species C II and N II. If the gas is distributed in a spherically symmetric shell about the star, the mass of gas carried away by the wind is

$$dM/dt \approx 4\pi D_{in} m_{atom} N v_\infty \quad (11)$$

Summing over all observed states of C II and N II and assuming the column densities and escape velocities in Table 2, we estimate  $dM(\text{N II})/dt = 3.5 \times 10^{-12} M_\odot/\text{yr}$  and  $dM(\text{C II})/dt = 2.8 \times 10^{-12} M_\odot/\text{yr}$  if  $D_{in} = 20$  AU. We can also estimate the N II mass loss rate from the momentum imparted to the gas by radiation pressure,

$$v_\infty \frac{dM(\text{N II})}{dt} = \frac{L_\lambda}{c} W_\lambda \quad (12)$$

If  $v_\infty = 28$  km/sec, we estimate  $dM(\text{N II})/dt = 1.5 \times 10^{-12} M_\odot/\text{yr}$ , consistent with the estimate made assuming that the N II is optically thin.

If the system is in a steady state, the wind observed around  $\sigma$  Her returns  $\sim 100 M_\oplus$  of gas during the lifetime of the system. Thus,  $\sigma$  Her depletes the mass in parent bodies in less than the estimated age of the star. Either the dust currently observed is produced in a short-lived stochastic event, or the system is in a steady state and the true parent body mass is probably well above the minimum we derive. For example, this mass could exist as meter-sized objects which are in stable orbits about the binary system and are difficult to detect in the mid infrared. At 20 AU, the estimated mass loss rate implies an

electron density,  $n_e \approx \dot{M}/(4\pi D_{in}^2 v_\infty m_{atom}) \approx 8.0 \text{ cm}^{-3}$  when summed over the observed species, suggesting that electron-atom collisions are only moderately significant in this environment.

## 6. DISCUSSION

Although the circumstellar gas around  $\sigma$  Her appears to be outflowing in a wind, the physical processes which generate the gas are uncertain. One possibility is that the gas is generated from the sublimation of comets, as observed around  $\beta$  Pic (Vidal-Madjar et al. 1994) and 51 Oph (Roberge et al. 2002). Another possibility is that the gas is produced through collisions between parent bodies. Here, we consider both models.

If orbiting comets produce the absorption features observed then there could be as many redshifted events as blueshifted events (Crawford, Beust, & Lagrange 1998). However, all of the absorption features observed toward  $\sigma$  Her are blueshifted. Furthermore, sublimation and subsequent photodissociation of water ice from comets should produce O I. No O I is observed in the *FUSE* spectrum of  $\sigma$  Her. Finally, we can estimate the distance at which comets sublime around  $\sigma$  Her assuming typical gravitational motions.

$$D_{sub} \sim \frac{GM_{tot}}{(\Delta v)^2} \quad (13)$$

where  $\Delta v$  is the observed line width in velocity units. For  $\sigma$  Her,  $D_{sub} = 9$  AU assuming  $M_{tot} = 4.5 M_\odot$  and  $\Delta v = 21$  km/sec neglecting radiative effects. This distance is thirty times further away than distance at which comets sublime around  $\beta$  Pic (Beust et al. 1998). In order to produce the same column density of absorbers, there must be 1000 times more comets around  $\sigma$  Her compared to  $\beta$  Pic (Beust, Karmann, & Lagrange 2001). The existence of so many comets around  $\sigma$  Her seems unlikely because the fractional infrared luminosity of  $\sigma$  Her is only 0.02 times that of  $\beta$  Pic.

Collisions between parent bodies may explain our data. 3-body orbits around  $\sigma$  Her are expected to become dynamically unstable at distances less than approximately three times the binary separation (Artymowicz & Lubow 1994). For  $\sigma$  Her, with a binary separation of 7 AU, this corresponds to  $\sim 20$  AU. Here, unstable orbits begin to cross each other, producing collisions between different objects. These collisions could provide a natural explanation for the generation of atomic gas from circumstellar matter. The high luminosity of the B9V primary then drives the gas from the circumstellar environment in a wind.

## 7. CONCLUSIONS

We have obtained an ultraviolet spectrum (between 905 Å and 1187 Å) of the nearby binary system  $\sigma$  Her using *FUSE*. We argue the following:

1. The ultraviolet spectrum of  $\sigma$  Her possess absorption in the excited fine structure lines of C II and N II. The excitation of these states and the narrow width of these absorption features suggest that the gas is circumstellar.

2. Since the Poynting-Robertson drag lifetime of dust grains at  $D_{in} = 20$  AU with  $a = 15 \mu\text{m}$  is  $4.6 \times 10^4$  yr, significantly shorter than the estimated age of  $\sigma$  Her, the

grains must be replenished from a reservoir such as collisions between larger objects. For  $\sigma$  Her, we estimate that the minimum mass of parent bodies is  $0.20 M_{\oplus}$ .

3. Because  $\sigma$  Her is a binary with a separation of 7 AU, parent body orbits become unstable at distances  $\sim 20$  AU from the system. Collisions of parent bodies at this distance could liberate gas which is then blown out of this system by the high luminosity of  $\sigma$  Her.

4. If the gas is released from grains at  $\sim 20$  AU from the star, then the predicted outflow velocities of C II\* and N II\*\* are  $\sim 31$  km/sec and  $\sim 26$  km/sec respectively, in rough agreement with the observed blueshifts of  $\sim 20$

km/sec and  $\sim 28$  km/sec respectively.

5. We infer a mass loss rate of  $dM/dt \sim 6 \times 10^{-12} M_{\odot}/\text{yr}$ , suggesting that  $\sigma$  Her depletes the mass in parent bodies in less than the estimated age of the system. This raises the likelihood that objects larger than  $\sim 1$  m are in orbit in this system.

This work has been supported by funding from NASA. We thank P. Chayer for providing us with a rotationally broadened synthetic spectrum for  $\sigma$  Her. We also thank A. Roberge for her comments and B.-G. Anderson for running our data through the CALFUSE 2.0.5 pipeline.

## REFERENCES

Abgrall, H., Roueff, E., Launay, F., Roncin, J.-Y., & Subtil, J.-L. 1993, A&AS, 101, 273

Artymowicz, P. 1988, ApJ, 335, L79

Artymowicz, P., & Lubow, S. H., 1994, ApJ, 421, 651

Beckwith, S. V. W., & Sargent, A. I. 1986, Nature, 383, 139

Beust, H., Lagrange, A.-M., Crawford, I. A., Goudard, C., Spyromilio, J., & Vidal-Madjar, A. 1998, A&A, 338, 1015

Beust, H., Karmann, C., & Lagrange, A.-M. 2001, A&A, 366, 945

Bruhweiler, F. C., Grady, C. A., & Chiu, W. A. 1989, ApJ, 340, 1038

Burns, J. A., Lamy, P. L., & Soter, S. 1979, Icarus, 40, 1

Cardelli, J. A., Clayton, G. C., & Mathis, J. S. 1989, ApJ, 345, 245

Chayer, P. 2001, personal communication

Chen, C. H., & Jura, M. 2001, ApJ, 560, L171

Coté, J. 1987, A&A, 181, 77

Crawford, I. A., Beust, H., & Lagrange, A.-M. 1998, MNRAS, 294, L31

Fajardo-Acosta, S. B., Stencel, R. E., & Backman, D. E. 1997, ApJ, 487, L151

Fajardo-Acosta, S. B., Telesco, C. M., & Knacke, R. F. 1998, ApJ, 115, 2101

Federman, S. R., Glassgold, A. E., & Kwan, J. 1979, ApJ, 227, 466

Figueras, F., & Blasi, F., 1998, A&A, 329, 957

Flower, P. J. 1996, ApJ, 469, 355

Grady, C. A., Bruhweiler, F. C., Cheng, K.-P., & Chiu, W. A. 1991, ApJ, 367, 296

Grosbøl, P. J. 1978, A&AS, 32, 409

Hartkopf, W. I.; McAlister, H. A., Mason, B. D., Brummelaar, T. T., Roberts, L. C., Jr., Turner, N. H., & Wilson, J. W. 1997, AJ, 114, 1639

Heap, S., Lindler, D. J., Lanz, T. M., Cornett, R. H., Hubeny, I., Maran, S. P., & Woodgate, B. 2000, ApJ, 539, 435

Hoffleit, D., & Warren, W. H. 1991, The Bright Star Catalogue (5th ed.; New Haven: Yale Univ. Obs.)

Holland, W. S., Greaves, J. S., Zuckerman, B., Webb, R. A., McCarthy, C., Coulson, I. M., Walther, D. M., Dent, W. R. F. et al. 1998, Nature, 392, 788

Hummel, C. et al. 2002, personal communication, data from Navy Prototype Optical Interferometer

Lagrange, A.-M., Beust, H., Mouillet, D., Deleuil, M., Feldman, P. D., Ferlet, R., Hobbs, L., Lecavelier des Etangs, A. et al. 1998, A&A, 330, 1091

Lecavelier des Etangs, A., Vidal-Madjar, A., Roberge, A., Feldman, P. D., Deleuil, M., André, M., Blair, W. P., Bouret, J.-C. et al. 2001, Nature, 412, 706

Low, F., Hines, D. C., & Schneider, G., 1999, ApJ, 520, L45

Martin, C., Mignard, F., Hartkopf, W. I., & McAlister, H. A. 1998, A&AS, 133, 149

Morton, D. C. 1991, ApJS, 77, 119

Morton, D. C., & Noreau, L. 1994, ApJS, 95, 301

Roberge, A., Feldman, P. D., Lecavelier des Etangs, A., Vidal-Madjar, A., Deleuil, M., Bouret, J.-C., Ferlet, R., & Moos, H. W. 2002, ApJ, 568, 343

Sadakane, K., & Nishida, M. 1986, PASP, 98, 685

Sahnou, D. J., Moos, H. W., Friedman, S. D., Blair, W. P., Conard, S. J., Kruk, J. W., Murphy, E. M., Oegerle, W. R. et al. 2000, SPIE, 4139, 131

Schneider, G. et al. 1999, ApJ, 513, L127

Spitzer, L. 1978, Physical Processes in the Interstellar Medium (New York: John Wiley & Sons, Inc.)

Vidal-Madjar, A., Lagrange-Henri, A.-M., Feldman, P. D., Beust, H., Lissauer, J. J., Deleuil, M., Ferlet, R., Gry, C. et al. 1994, A&A, 290, 245

Weinberger, A. J., Becklin, E. E., Schneider, G., Smith, B. A., Lowrance, P. J., Silverstone, M. D., Zuckerman, B., & Terrile, R. J. 1999, ApJ, 525, L53

TABLE 1  
 $\sigma$  HER PROPERTIES

Quantity	Adopted Value	Reference
Primary Spectral Type	B9V	1
Distance	93 pc	2
Effective Temperature ( $T_{eff}$ )	10,500 K	
Stellar Radius ( $R_*$ )	4.6 $R_\odot$	
Stellar Luminosity ( $L_*$ )	230 $L_\odot$	
Total Binary Mass ( $M_{tot}$ )	4.5 $M_\odot$	3
Rotational Velocity ( $v \sin i$ )	270 km/sec	1
Fractional Dust Luminosity ( $L_{IR}/L_*$ )	$6.6 \times 10^{-5}$	4
Estimated Age	140 Myr	
Inner Grain Temperature	240 K	4
Inner Dust Distance ( $D_{in}$ )	20 AU	
Outer Grain Temperature	100 K	
Outer Dust Distance ( $D_{out}$ )	120 AU	
Minimum Parent Body Mass ( $M_{PB}$ )	0.20 $M_\oplus$	

References. — (1) Hoffleit & Warren (1991); (2) *Hipparcos*; (3) Martin et al. (1998); (4) Fajardo-Acosta et al. (1998)

TABLE 2  
 PROPERTIES OF CIRCUMSTELLAR GAS

Species	Wavelength (Å)	Ground State Energy (cm <sup>-1</sup> )	$W_\lambda^{\dagger}$ (mÅ)	$N^{\ddagger}$ (10 <sup>14</sup> cm <sup>-2</sup> )	Observed $v_\infty$ (km/sec)	Predicted $v_\infty^{\ddagger}$ (km/sec)	$\beta$
C II	1036.34	0.00	$184 \pm 12$	4.1	-16	-29	3.2
C II*	1037.02	63.42	$222 \pm 14$	8.2	-20	-31	3.4
N II	1083.99	0.00	$109 \pm 10$	$\geq 1.0$	-14	-24	2.5
N II*	1084.58	48.67	$158 \pm 17$	$\geq 1.5$	-28	-24	2.5
N II**	1085.54	130.8	$114 \pm 12$	$\geq 6.7$	-25	-26	2.7
N II**	1085.70	130.8	$221 \pm 21$	$\geq 2.5$	-28	-26	2.7
O I*	1040.94	158.27	$\leq 39$	$\leq 4.5$	N/A		
O I**	1041.69	226.98	$\leq 31$	$\leq 3.5$	N/A		
H <sub>2</sub> (J=0)	1036.54	0.00	$\leq 95$	$\leq 4$	N/A		
H <sub>2</sub> (J=1)	1038.16	118.16	$\leq 54$	$\leq 7$	N/A		
CO (J=2)	1088.05	11.58	$\leq 75$	$\leq 1$	N/A		
CO (J=4)	1087.73	38.61	$\leq 70$	$\leq 1$	N/A		

<sup>†</sup>error bars are statistical uncertainties in the measurement of the equivalent width and do not account for uncertainty in continuum fitting

<sup>‡</sup>C II column densities, predicted outflow velocities, and  $\beta$ s are corrected for optical depth assuming that the gas is at the edge of the cloud. N II is assumed to be optically thin.

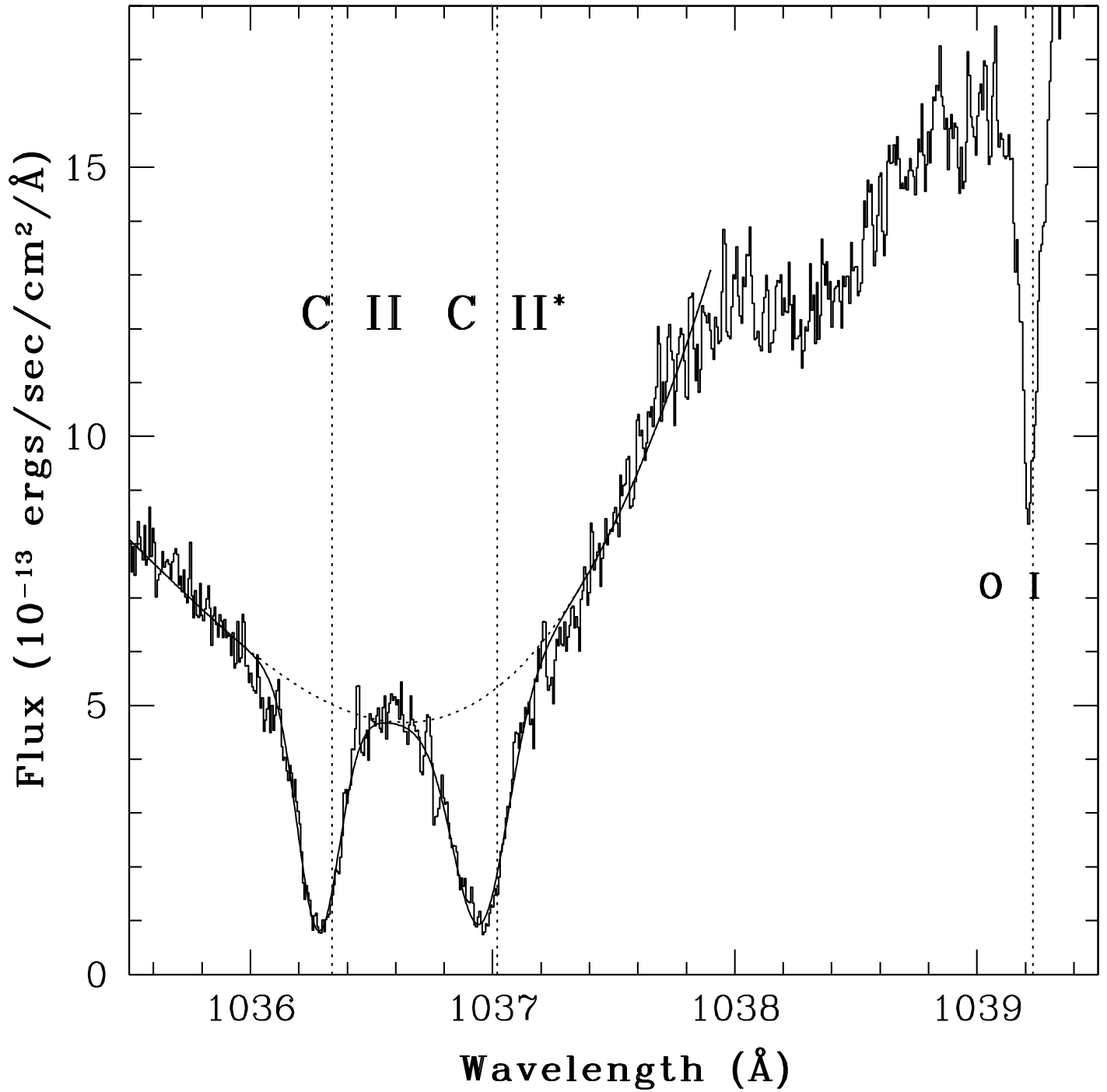


FIG. 1A.— The circumstellar C II  $\lambda$  1037 doublet and interstellar O I  $\lambda$  1039 line. The solid curve is a minimum  $\chi^2$  fit to the C II doublet using Gaussians to model the photospheric and circumstellar components. The dotted curve shows the photosphere model. The vertical lines indicate wavelengths of the C II, C II\*, and O I lines at the star's velocity.

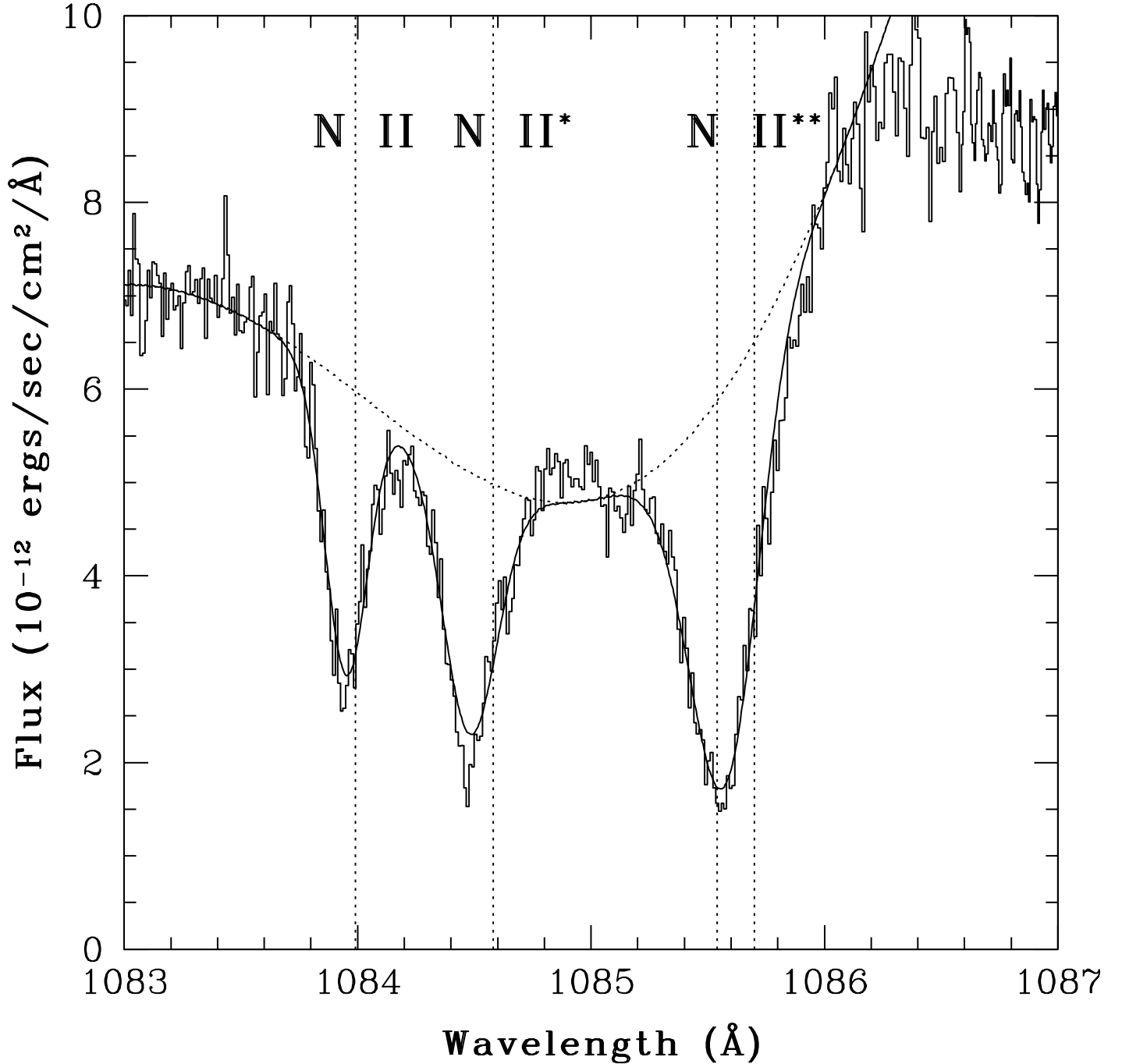


FIG. 1B.— The circumstellar N II  $\lambda$  1085 multiplet. The solid curve is a minimum  $\chi^2$  fit to the N II multiplet using Gaussians to model the photospheric and circumstellar components. The dotted curve shows the photosphere model. The N II\* and N II\*\* lines are a doublet and triplet respectively whose components are blended together. The vertical lines indicate the wavelength of the N II line, the average wavelength of the N II\* doublet, and the wavelengths of the N II\*\* lines with the largest f-values at the star's velocity.

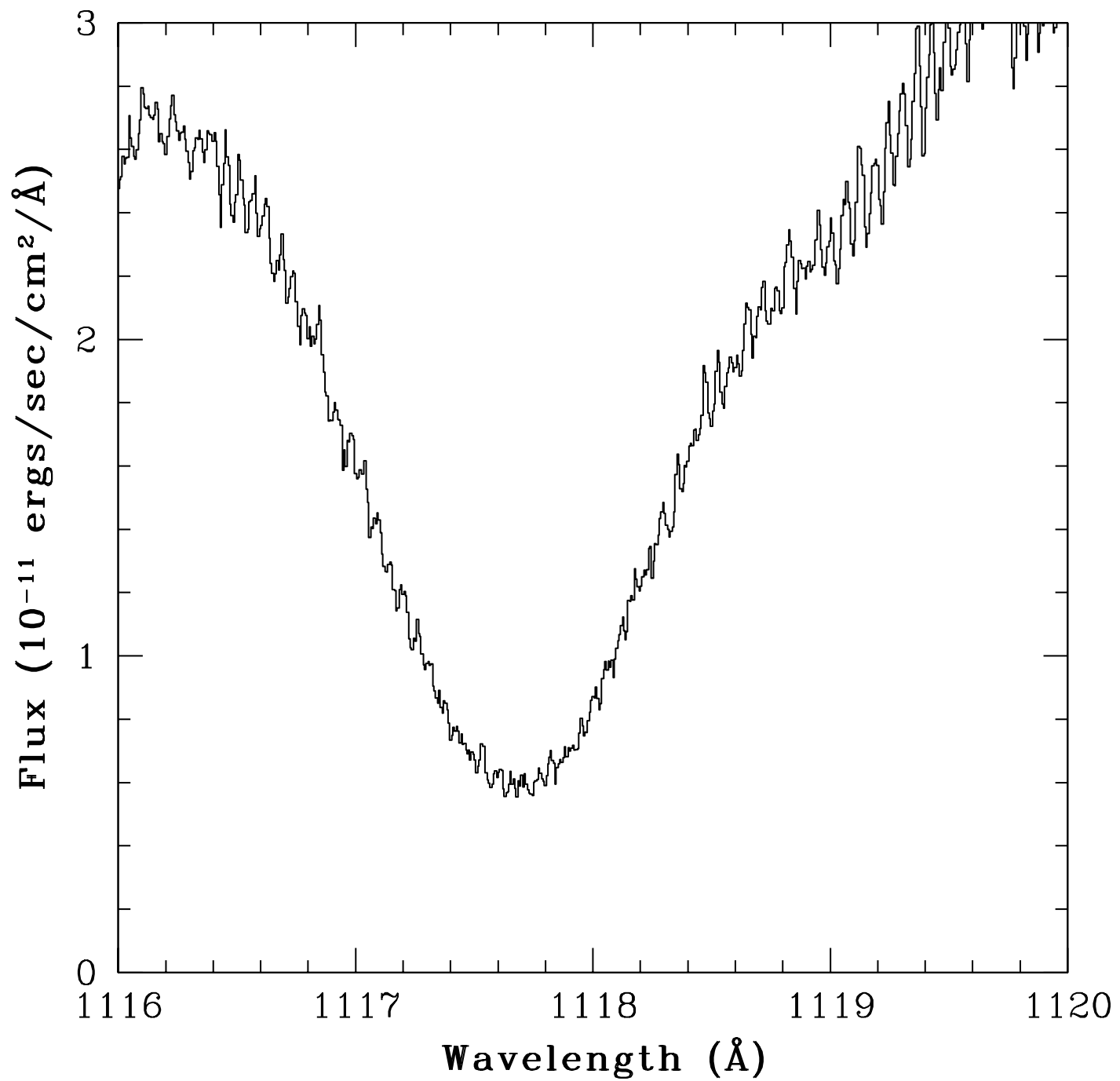


FIG. 1C.— The stellar C I  $\lambda$  1118 line.